

UNCLASSIFIED

AD NUMBER

ADB029195

LIMITATION CHANGES

TO:

Approved for public release; distribution is unlimited.

FROM:

Distribution authorized to U.S. Gov't. agencies only; Test and Evaluation; JUN 1978. Other requests shall be referred to Naval Weapons Center, China Lake, CA.

AUTHORITY

NWC ltr 1 Oct 1979

THIS PAGE IS UNCLASSIFIED

THIS REPORT HAS BEEN DELIMITED
AND CLEARED FOR PUBLIC RELEASE
UNDER DOD DIRECTIVE 5200.20 AND
NO RESTRICTIONS ARE IMPOSED UPON
ITS USE AND DISCLOSURE.

DISTRIBUTION STATEMENT A

APPROVED FOR PUBLIC RELEASE;
DISTRIBUTION UNLIMITED.

NWC TP 6029

9

AD B029195

LEVEL II

PW

Design Study for a 100-Watt Turboalternator Power Unit

by
Dr. O. E. Balje
and
R. Spies
Dr. O. E. Balje, Inc.
for the
Ordnance Systems Department

JUNE 1978



Distribution limited to U.S. Government agencies only; test and evaluation; 31 May 1978. Other Requests for this document must be referred to the Naval Weapons Center.

DDC FILE COPY

Naval Weapons Center

CHINA LAKE, CALIFORNIA 93555

78 08 08 037



Naval Weapons Center

AN ACTIVITY OF THE NAVAL MATERIAL COMMAND

FOREWORD

This report deals with the optimization of a compressed gas 100-watt turboalternator power unit designed for potential use aboard an expendable electronic countermeasures unit. This investigation was conducted from September 1977 to February 1978. The work was sponsored by the Naval Weapons Center (NWC), China Lake, California, under Navy Contract N60530-77-M-400T and supported by the Naval Air Systems Command jointly through the ZEPPO program, AirTask AIR-350-350F/008C/7W0645-001, and the Advanced Power Supplies Program, AirTask A03W3300/008B/7F31300000.

Mr. Steven E. Ayler was the NWC technical coordinator and has reviewed this report for technical accuracy.

This report is released for information at the working level and does not necessarily reflect the views of NWC.

Approved by
P. E. CORDLE, Head (Acting)
Ordnance Systems Department
30 May 1978

Under authority of
W. L. HARRIS
RAdm., U.S. Navy
Commander

Released for publication by
R. M. HILLYER
Technical Director

NWC Technical Publication 6029

Published by	Technical Information Department
Collation	Cover, 19 leaves
First printing	120 unnumbered copies

UNCLASSIFIED

~~SECURITY~~ CLASSIFICATION OF THIS PAGE (When Data Entered)

REPORT DOCUMENTATION PAGE		READ INSTRUCTIONS BEFORE COMPLETING FORM	
NWC TP-6029		2. GOVT ACCESSION NO.	3. RECIPIENT'S CATALOG NUMBER
4. TITLE (and subtitle)		5. TYPE OF REPORT & PERIOD COVERED	
DESIGN STUDY FOR A 100-WATT TURBOALTERNATOR POWER UNIT		Final report Start 77-Feb-1978	
6. PERFORMING ORG. REPORT NUMBER		7. CONTRACT OR GRANT NUMBER(S)	
O. E. Balje R. Soles		N60530-77-M-400T/nsw	
8. PERFORMING ORGANIZATION NAME AND ADDRESS (O. E. Balje, Inc. 14724 Ventura Blvd. Sherman Oaks, California 91413		9. PROGRAM ELEMENT, PROJECT, TASK AREA & WORK UNIT NUMBERS SIC 050475 AIR-350-350F/008C/7W0645-001 A03W-3300/008B/7F31300000	
10. CONTROLLING OFFICE NAME AND ADDRESS Naval Weapons Center China Lake, California 93555		11. NUMBER OF PAGES 36	
12. MONITORING AGENCY NAME & ADDRESS (if different from Controlling Office) F31380		13. SECURITY CLASS. (of this report) UNCLASSIFIED	
14. DISTRIBUTION STATEMENT (of the abstract entered in Block 20, if different from Report) Distribution limited to U.S. Government agencies only; test and evaluation; May 1978. Other requests for the document must be referred to the Naval Weapons Center.		15. DECLASSIFICATION/DOWNGRADING SCHEDULE 12/39	
16. DISTRIBUTION STATEMENT (of the abstract entered in Block 20, if different from Report)			
17. DISTRIBUTION STATEMENT (of the abstract entered in Block 20, if different from Report)			
18. SUPPLEMENTARY NOTES			
19. KEY WORDS (Continue on reverse side if necessary and identify by block number) Power Supply Helium Turboalternator Nitrogen Turbine High Speed Bearings Terry Turbine			
20. ABSTRACT (Continue on reverse side if necessary and identify by block number)			
See reverse side of this form.			

DD FORM 1 JAN 73 1473

EDITION OF 1 NOV 65 IS OBSOLETE
S/N 0102-014-6601

UNCLASSIFIED

SECURITY CLASSIFICATION OF THIS PAGE (When Data Entered)

UNCLASSIFIED

SECURITY CLASSIFICATION OF THIS PAGE(When Data Entered)

(U) *Design Study for a 100-Watt Turboalternator Power Unit*, by Dr. O. E. Balje and R. Spies, Dr. O. E. Balje, Inc. China Lake, Calif., Naval Weapons Center, June 1978, 36 pp. (NWC TP 6029, publication UNCLASSIFIED.)

(U) The design of a 100-watt turboalternator is investigated. Three turbine types are considered: Terry, Terry with re-entry, and side Terry with simplified buckets. Two compressed gases are considered: helium and nitrogen. Various high speed bearings are considered, with deep groove radial ball bearings, angular contact ball bearings, and three-lobe journal bearings discussed in detail. Two alternator types are considered, flux switch and rotating magnet.

(U) Turbine design details for the highest efficiency helium and nitrogen systems are determined, and their gas storage requirements are compared with the desired storage volume.

UNCLASSIFIED

SECURITY CLASSIFICATION OF THIS PAGE(When Data Entered)

CONTENTS

Introduction	3
Design Specifications	3
Analysis	4
Helium System	4
Scope of Investigation	4
Alternator Performance Trends	4
Bearing Investigations	6
Turbine Performance	16
Unit Performance	20
Nitrogen System	29
Scope of Investigations	26
Unit Performance	29
Summary	35
Helium System	35
Nitrogen System	35

ACCESSION for	
NTIS	White Section <input type="checkbox"/>
DDC	Buff Section <input checked="" type="checkbox"/>
UNANNOUNCED <input type="checkbox"/>	
JUSTIFICATION _____	
BY _____	
DISTRIBUTION/AVAILABILITY CODES	
Dist.	All. And/or SPECIAL
<i>B</i>	

1 78 08 08 037

INTRODUCTION

This report describes the investigations performed for optimizing the turbine and bearing design of a 100-watt turboalternator power unit driven by compressed gas. It is part of a study by NWC to determine the technical and economic feasibility of using a compressed gas turboalternator power supply aboard an expendable electronic countermeasures unit. Since the application is volume limited, ultra-high gas storage pressure (25,000 psi, 172 MPa) will be used to improve the energy density, and maximum energy conversion efficiency will be a goal in the turboalternator design. Because the unit is expendable, low overall cost is also a critical design requirement.

As a compressed gas is slowly released from a storage reservoir, the temperature of the stored gas decreases steadily due to isentropic expansion. Since this results in a loss of energy storage capability, and causes unsteady turboalternator operation, heat will be transferred to the stored gas via slow burning pyrotechnics at a rate which produces a constant reservoir exhaust temperature. As a result of Joule-Thomson heating, the initial exhaust temperature will be above the storage temperature and thus will define the constant nozzle inlet stagnation temperature shown in the following specifications.

Two gases, helium and nitrogen, were investigated since they represent high volumetric performance and low cost systems, respectively.

DESIGN SPECIFICATIONS

- A. Working fluid: gaseous helium or nitrogen
- B. Gas storage pressure: 25,000 psi (172 MPa)
- C. Gas storage volume: 100 in³ (1.64 liters)
- D. Alternator
 - 1. Output power: 100 watts
 - 2. Output frequency: 20 kHz
 - 3. Configuration
 - a. Helium system: rotating magnet (ultra high speed)
 - b. Nitrogen system: flux switch (50,000-60,000 rpm)
- E. Stagnation pressure at nozzle inlet: 1,000 psi
- F. Stagnation temperature at nozzle inlet
 - 1. Helium system: 250°F (121°C)
 - 2. Nitrogen system: 160°F (71°C)
- G. Turbine exhaust pressure: 5.5-14.7 psia (34,500-101,400 Pa)
- H. Operating time: 20 minutes
- I. Desired turboalternator efficiency:
 - 1. Helium system: 30%
 - 2. Nitrogen system: 50%

ANALYSIS

HELIUM SYSTEM

Scope of Investigation

A brief review of the specifications shows that extremely high rotative speeds (in excess of 150,000 rpm) will be desired to obtain the required turbine efficiency. This trend is likely to be counteracted by bearing and alternator performance considerations. Thus, a trade-off study is desired so that the analysis will have to deal with the performance trends in turbines, bearings, and alternators. For cost reasons, only single-rotor turbines are considered. Antifriction bearings and gas lubricated bearings are investigated as bearing candidates, whereas, for alternator performance the technical data supplied by two companies (Simmonds Precision and Varo) specializing in low powered high speed alternators and the data of AFAPL-TR-76-44¹ have been used.

Alternator Performance Trends

Most small alternators are designed for rotative speeds of 60,000 rpm and below. This seems to be the operating regime where the most design know-how exists and where fairly firm quotations can be obtained for the obtainable efficiencies. They range from 75-80% when windage losses are included. Low powered alternators have been built for speeds of 200,000 rpm and above but performance data for these designs are not available.

Simmonds Precision lists a 15-watt 200,000 rpm alternator unit with a rotor which is 0.69 inch in diameter and 0.1875 inch long. Extrapolating to 100 watts, and allowing for added losses due to that extrapolation, results in a rotor length of about 1.5 inches. The Air Force 60-watt unit (footnote 1) obtained, by actual test, 42.4 watts at 181,000 rpm (close to the present design speed of 200,000 rpm) with a rotor which was smaller. An electrical efficiency (excluding windage losses) of 85% was deduced from the test data. One difference between the two units which may be significant is that the 60-watt unit was a two-pole platinum-cobalt machine, while the Simmonds Precision unit had a samarium cobalt rotor, which appears to have 8 poles. This affects frequency and losses to some extent. Also, the 60-watt design was dominated by a need to keep conducted heat from the magnet, something which will not be necessary here.

¹ J. A. Speeds and R. Spies. 60-Watt Power Source. Eglin Air Force Base, Florida, April 1976.
(AFAPL-TR-76-44.)

At any rate, the rotor will be approximately 0.5-0.7 inch in diameter and no more than 1.5 inches long for a 200,000 rpm unit.

It would appear, therefore, that the assumption of an electrical efficiency of 85% is justified for high speed alternators and that the overall alternator efficiency differs from this value only by the windage losses. An approximate value for these losses is obtained when it is assumed that the rotor for a 200,000 rpm unit has a diameter of about 0.5-0.7 inch and a length of about 1.25-1.5 inches.

The windage losses are calculated by the relation

$$HP = \frac{u^3 D^2 \gamma}{g 550} (\lambda_w + \frac{\pi}{4} \frac{1}{D} \lambda_R) \quad (1)$$

when λ_R denotes a friction coefficient for the cylindrical portion of the rotor which depends on the Taylor number defined as

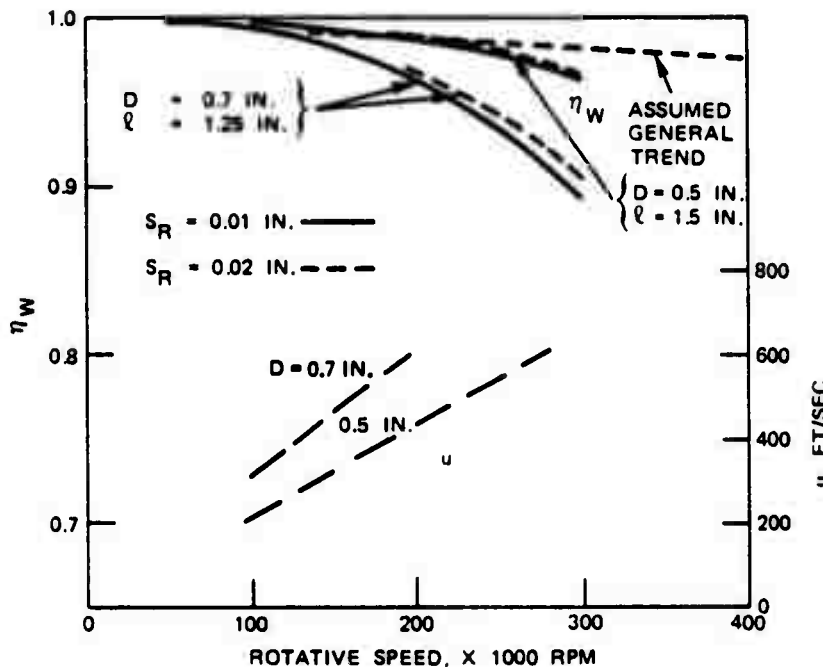
$$T_a = \frac{us_R}{\nu} \sqrt{\frac{2s_R}{D}} \quad (2)$$

The symbol λ_w denotes the friction coefficient of the end sections which depends on the peripheral Reynolds number defined as

$$R_e * = \frac{Du}{\nu} \quad (3)$$

In Equations 1 through 3, D denotes the rotor diameter, l the rotor length, u the rotor tip speed, s_R the radial clearance, ν the kinematic viscosity and γ the density of the medium surrounding the rotor. Typical data resulting from these relations are plotted in Figure 1 by presenting a *windage efficiency* as a function of rotative speed for two different rotor configurations and radial gaps of 0.01 and 0.02 inch. This diagram shows that a 0.5-inch-diameter rotor will be preferable and that the size of the air gap is not a decisive criterion. A windage efficiency of 99% is shown for the 0.5-inch-diameter rotor for a rotative speed of 200,000 rpm and a windage efficiency of about 96% for the 0.7-inch-diameter rotor. Increasing the rotative speed to 250,000 rpm, a windage efficiency of 98% is shown for the 0.5-inch rotor. These data show that small diameter rotors will be preferred to reduce windage losses. Assuming that the rotor diameter can be reduced to less than 0.5 inch for $N > 200,000$ rpm, the dotted line in Figure 1 would represent the trend for the *windage efficiency*.

The lower section of Figure 1 shows the rotor tip speed as a function of rotative speed for the two diameters. A tip speed value of 600 ft/s appears to be currently used in small high-speed alternators. Thus, a 0.7-inch-diameter rotor can be used up to 200,000 rpm and a 0.5-inch-diameter rotor up to rotative speeds of 275,000 rpm.

FIGURE 1. Windage Efficiency (η_w) of Alternators.

Bearing Investigations

Two types of bearings were considered for use in the power source—journal and ball bearings. In each case, very small size and high-speed operation were the prime design constraints. For the journal bearings, three-lobe pressurized, and hydrodynamic designs were reviewed.

Bearing Size and Load Estimates. To analyze the bearings for this short-life but high-speed application, it is important to determine the bearing size which might be used. From data made available by manufacturers of alternators and from the experience of the author with the Air Force 60-watt alternator rotor (footnote 1), it can be concluded that bearings with a bore as small as 0.125 inch can be used.

Bearing loads will influence operation. Such loads will result from gravity forces (weight of the rotor), which may be in any direction, and electrical/magnetic loads due to the magnetic field when current is generated.

Rotor weight is estimated to be less than 0.2 lb; therefore, the bearing load should be about 0.1 lb per bearing. Magnetic loads are not known, but for design purposes an equal load has been assumed.

Critical Speed Consideration. Two types of critical speeds must be considered. The first is that of the rotor. Because the rotor is extremely stiff, this critical speed

will be very large. The second is the speed at which the film in a fluid film bearing becomes unstable, resulting in a breakdown of the ability of the film to carry the load. For various bearings, this value is different.

The plain hydrodynamic journal bearing usually reaches critical speed at a relatively low rpm, governed predominantly by the clearance. For pressurized journal bearings, more stability results because of the greater stiffness of the film and smaller clearances. The three-lobe bearing has the most stability because the placement of the radii of curvature to be offset from each other provides a natural wedge action in the bearing. Stability will be discussed separately for each bearing.

Ball Bearings. Ordinarily, ball bearings are limited by their life expectancy. In this application, life requirements are very short, so that some liberties with bearings design can be taken.

Types of Ball Bearings. For this application where high speed, small size and low loads predominate, two types of ball bearings were considered:

1. Deep groove radial bearings with a reinforced phenolic, one-piece, machined, side-assembled cage
2. Angular contact bearings with one-piece phenolic cage, outer-ring pivoted

Both of these bearing types provide radial as well as thrust load capability. They can be obtained from various manufacturers but for convenience only, data supplied by the Barden Corporation has been used in this analysis.²

The bearings selected for analysis and their characteristics are:

Bearing type	Bearing no.	Diameter, in.		Width, in.	Limiting speed, rpm	Performance constraints (see footnote 2)				
		Bore	OD			c, lb	F _r	F _t	M _C , g-cm	F _v , × 10 ⁶
Deep groove	SR144STAX3	0.125	0.250	0.0937	163,000	38	1.45	1.75	0.024	0.88
Angular contact	SR2-5B	0.125	0.312	0.1094	242,000	63	1.30	2.05	0.035	1.70

While the limiting speed for the deep-groove bearings is below the operating speed of 200,000 rpm, this is probably all right because of the short life requirement. As stated later, the limiting dN value indicates a safe speed of 190,000 rpm. The Air Force 60-watt unit used these bearings successfully.

The angular contact bearing, while rated at a higher speed, requires more power to operate.

²Barden Corporation, Danbury, Connecticut, Catalog M6.

Bearing Life. For estimating purposes, bearing life (hours) can be expressed as

$$L = A_1 A_2 \frac{16666}{N} \left(\frac{c}{P} \right)^3$$

where

A_1 = Life reliability factor, 0.11 for a 99% survival rate (very conservative)

A_2 = Life modifying factor, 3.0 per manufacturer's data

c = Basic dynamic load rating

38 for deep groove bearing

65 for angular contact bearing

P = Load, 0.2 lb

Therefore, L will be in excess of 60,000 hours. Obviously, life will not be a major consideration in the design.

Bearing Lubricant. For simplicity, and because operating time is short, a grease packed bearing is suggested. The type of grease must be of very high quality, such as Beacon 325, which can be used over a temperature range of -65 to +250°F. To achieve full elastohydrodynamic film in the bearing, a minimum viscosity is required. It is given by

$$\nu = \frac{5 \times 10^7}{cN}$$

where C = clearance and N = rotating speed, and is calculated to be less than 7 centistokes. Grease viscosity is estimated to be between 10 and 20 centistokes at operating temperatures.

Speed Limitations. For petroleum base greases, a limiting speed value is that the rpm multiplied by the bearing bore diameter in millimeters (the so-called dN value) should not exceed 600,000. At 200,000 rpm, a 3 mm or 0.118-inch-diameter bore is usable. At a bore of 0.125 inch, the dN value is 635,000, and this diameter is probably all right considering the short life and low loads being used.

Bearing Torque. Most important in the design is the amount of power the bearings will dissipate. Four components make up the dissipating torque:

Torque due to radial load

Torque due to thrust load

Static torque due to cage weight

Dynamic torque due to viscous shear of lubricant

Torque due to radial and thrust loads will be extremely small because of the low load values, probably on the order of 0.01 g-cm each. Static torque also is small, being 0.024 for the deep-groove bearing and 0.045 for the angular contact bearing. Dynamic

NWC TP 6029

torque is really the only one which must be considered in detail. It is calculated by using

$$M_v = (F_v N \nu)^{2/3}$$

where

$$\begin{aligned} F_v &= \text{performance constant} \\ &\quad 0.88 \times 10^6 \text{ for deep groove bearing} \\ &\quad 1.7 \times 10^6 \text{ for angular contact bearing} \\ N &= 200,000 \text{ rpm} \\ \nu &= 20 \text{ centistokes (estimated)} \end{aligned}$$

Therefore, the torque is 2.3 g-cm for the deep-groove and 3.6 g-cm for the angular contact bearing. Power absorption at 200,000 rpm is, therefore, 4.7 and 7.4 watts per bearing, respectively.

This would indicate the desirability of using a less viscous oil instead of grease. The Air Force 60-watt unit was operated with a low viscosity oil. The element which enters this tradeoff is the storage capability. If long-term storage is required, grease will be more reliable. If shelf life is reasonably short, oil can be loaded into the bearing at assembly. A design where oil is supplied to the bearing during operation by a wick from a reservoir is also feasible, but more complicated. If viscosity is cut in half, power losses will reduce to 3.0 and 4.7 watts per bearing, respectively. Figure 2 shows the power absorption of a deep-groove bearing as a function of speed for two different viscosities, $\nu = 20$ and 10 centistokes, respectively.

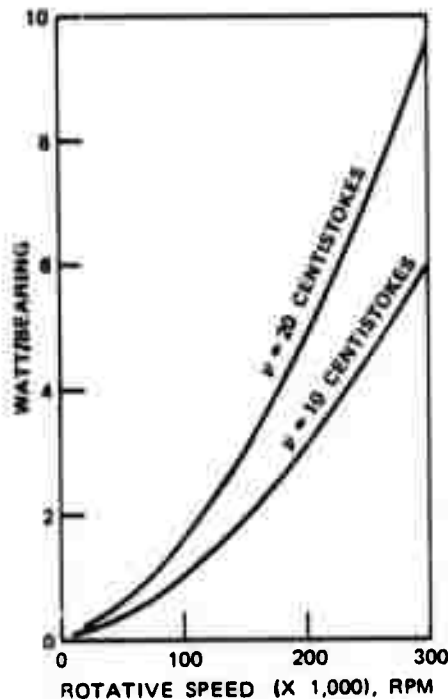


FIGURE 2. Power Absorption of Deep Groove Ball Bearing.

Three-Lobe Bearing. The three-lobe bearing, Figure 3, is inherently a stable bearing. Because of its geometry, even when the journal is centered, there is a wedge action in the film resulting in a loaded condition. Therefore, the stability threshold is raised and the bearing operates at low or even zero eccentricity.

AFAPL-TR-65-45³ was used in formulating the analysis. The curves shown in Figures 4 through 9 were taken from this report. Key parameters are:

Reynolds number	$\frac{\rho R \omega C}{\mu}$
Sommerfeld number	$\frac{\mu N' D L}{W} \left(\frac{R}{C} \right)^2$
Stability parameter	$\frac{CM \omega^2}{W}$
Friction factor	$\frac{R}{C} \frac{F_t}{W}$
Dimensionless flow	$\frac{Q}{N' D L C}$
Preload	$\frac{r}{C}$

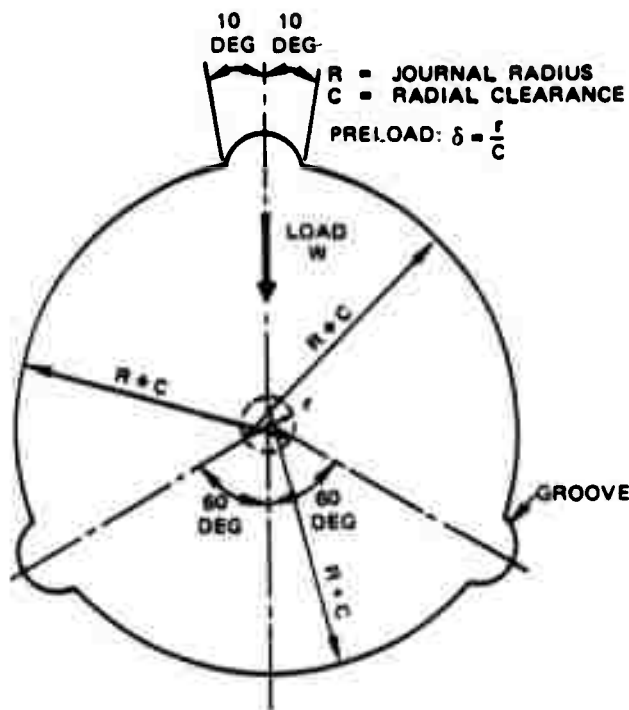


FIGURE 3. The Three-Lobe Bearing Schematic.

³ J. Lund, *Rotor-Bearing Dynamics Design Technology, Part VII*, Eglin Air Force Base, Florida, February 1968. (AFAPL-TR-65-45, Part VII.)

NWC TP 6029

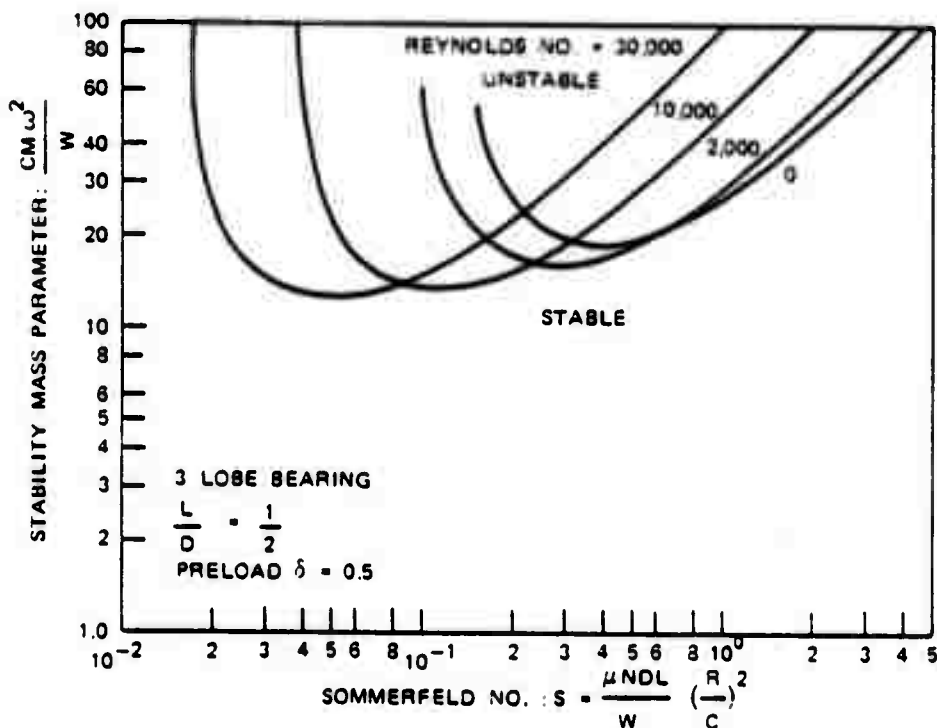


FIGURE 4. Three-Lobe Bearing Stability Map (Preload = 0.5, L/D = 1/2).

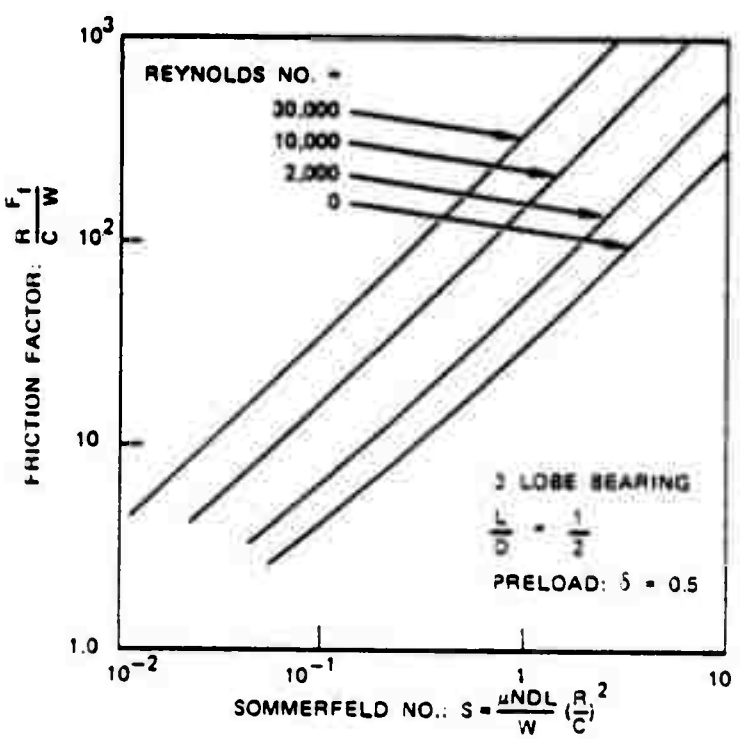


FIGURE 5. Three-Lobe Bearing Friction (Preload = 0.5, L/D = 1/2).

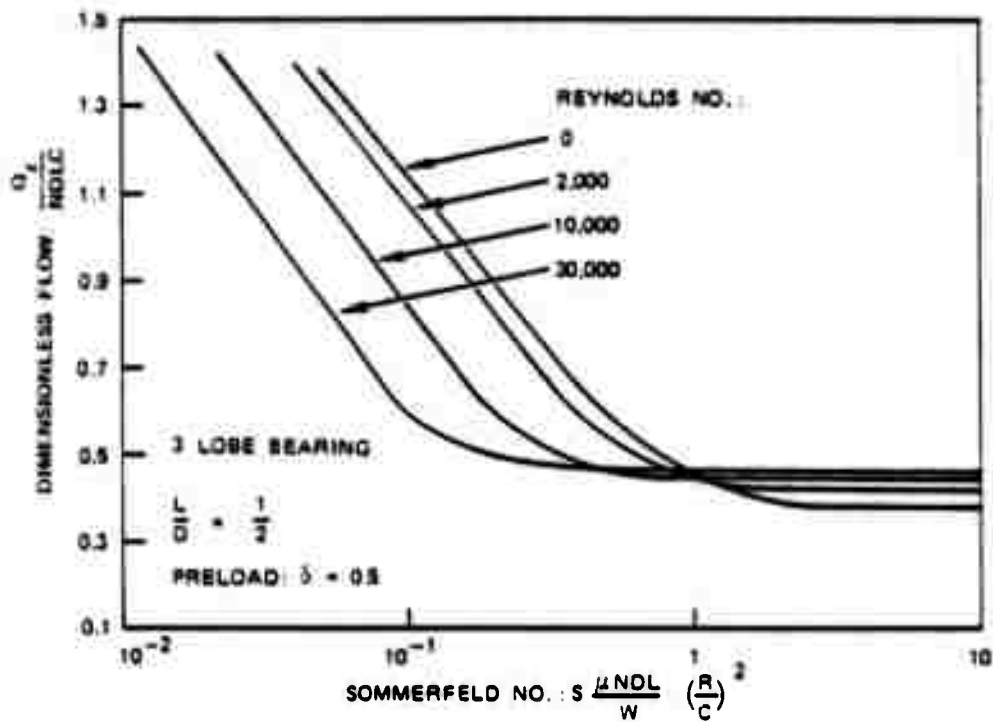


FIGURE 6. Three-Lobe Bearing Flow (Preload = 0.5, L/D = 1/3).

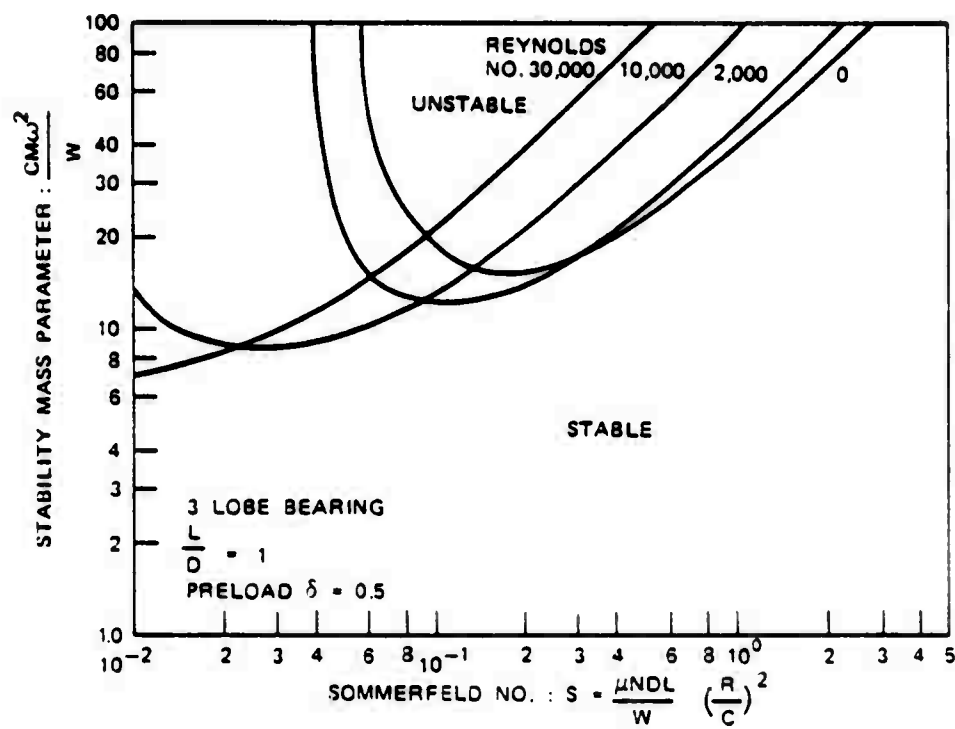


FIGURE 7. Three-Lobe Bearing Stability Map (Preload = 0.5, L/D = 1).

NWC TP 6029

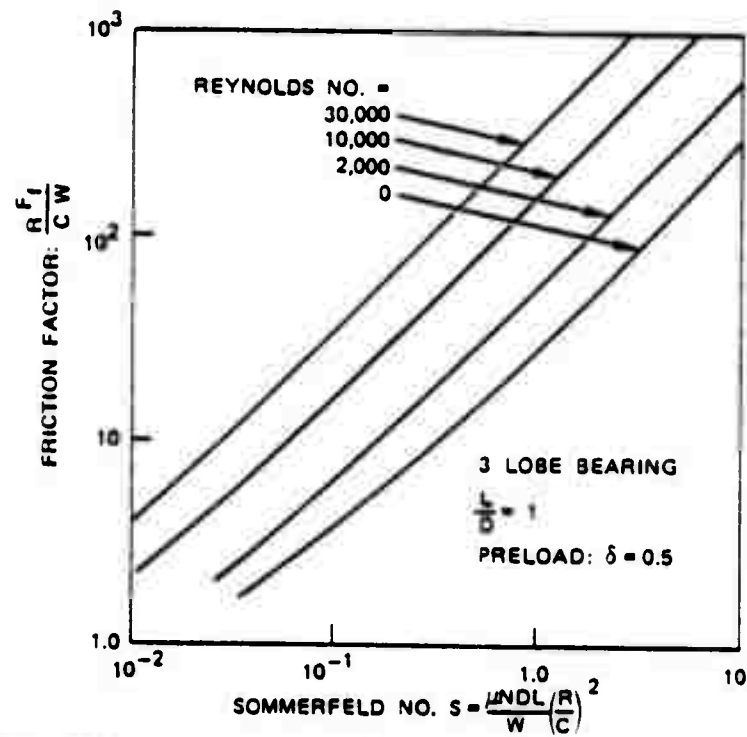


FIGURE 8. Three-Lobe Bearing Friction (Preload = 0.5, L/D = 1).

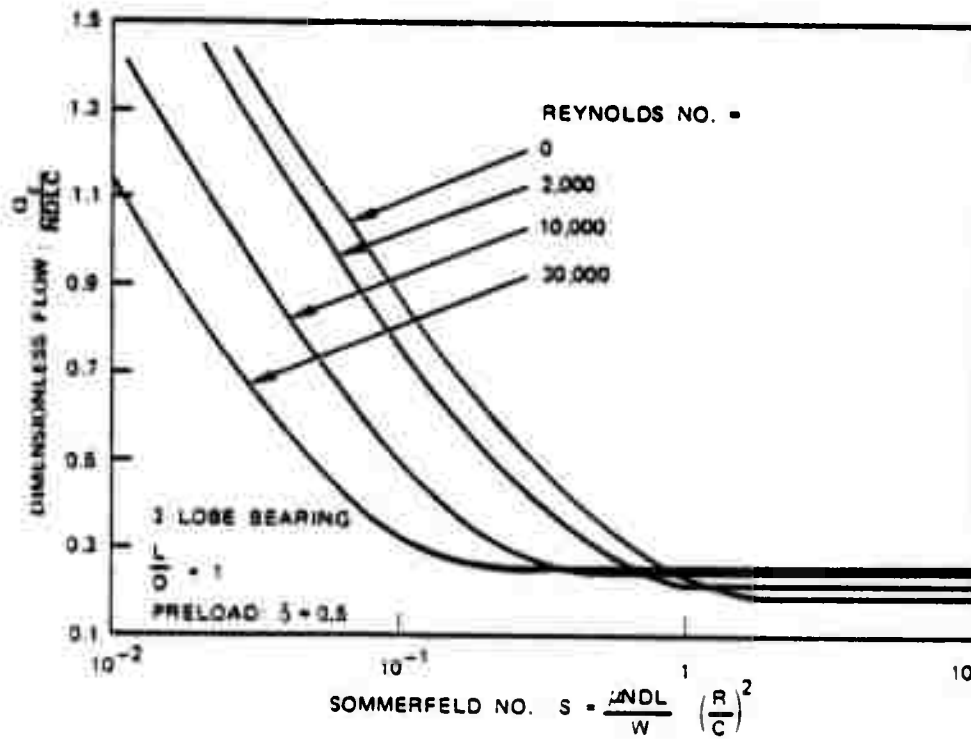


FIGURE 9. Three-Lobe Bearing Flow (Preload = 0.5, L/D = 1).

NWC TP 6029

where (conditions assumed for the analysis are in parentheses)

- ρ = gas density (0.21 lb/ft^3)
- R = journal radius (0.0625 in.)
- ω = angular speed of rotor ($20,944 \text{ rad/s}$)
- C = clearance (to be determined)
- μ = viscosity ($4.2 \times 10^{-9} \text{ lb-sec/in}^2$)
- N' = rotative speed (3,333 rps)
- D = journal diameter (0.125 in.)
- L = journal length (0.0625 in.)
- M = journal mass ($2.59 \times 10^{-4} \text{ lb-sec}^2/\text{in.}$)
- F_f = friction force
- Q = flow of gas
- r = offset of centers
- W = 0.1 lb

Using these values we get:

$$\begin{aligned}\text{Reynolds number} &= 98125 C \\ \text{Sommerfeld number} &= 4.27 \times 10^{-9}/C^2 \\ \text{Stability parameter} &= 11.36 \times 10^5 C \\ \text{Friction factor} &= 0.625 F_f/C \\ \text{Dimensionless flow} &= Q/26.0 C\end{aligned}$$

The Reynolds number, at any reasonable C , will be less than 100, and the curves for O can be used without serious error.

Referring to Figure 4, it is evident that if the stability parameter is less than 19, the bearing is stable no matter what the Sommerfeld number may be. Solving for C yields 1.67×10^{-5} inch, a very unrealistic value. Conversely, if Sommerfeld number is held below 0.15, stability is achieved at large stability parameter values. Solving again, $C = 1.69 \times 10^{-4}$ inch minimum. Larger values are okay. For analytical purposes, setting values at 0.001, 0.0005 and 0.000169 yields the results in Table 1, for which the data in Figure 5 were used to obtain F_f and in Figure 6 to obtain Q .

TABLE 1. Power Dissipation and Flow, Three-Lobe Bearing, $L/D = 1/2$.

Clearance, in.	0.001	0.0005	0.000169
Sommerfeld number	4.27×10^{-3}	0.0171	0.15
$(R/C)(F_f/W)$	0.4	1.2	6.0
F_f , lb	6.4×10^{-4}	9.6×10^{-4}	16.2×10^{-4}
$F_f R N$, watt	0.095	0.142	0.240
$Q/N D L C$	2.35	1.26	1.0
Volume of helium gas at 400 psi, in^3	73.2	19.7	5.27
Volume of helium gas at 25,000 psi, in^3	1.17	0.32	0.084
Available volume (2 bearings), %	3.3	0.65	0.17

A similar analysis can be made for a longer bearing using Figure 7. In that case, C minimum is 3.94×10^{-4} inch and again larger values are okay. Table 2 presents the power dissipation and flow data based on data in Figures 8 and 9.

These two tables indicate that three-lobe bearings will have low power dissipation under stable conditions and with reasonable gas flow if built-in clearances can be maintained below 0.001 inch. This may present something of a fabrication problem considering that the diameter is only 0.125 inch. The Air Force 60-watt unit had three-lobe bearings which were shaped by electric discharge machining. Such a technique may work here.

Plain Hydrodynamic Journal Bearing. The simplest journal bearing operates when the journal takes an eccentric position in the sleeve resulting in a film wedge. Instability will develop at about 15,000 rpm if the clearance is 0.001 inch. Reducing clearance to 0.0005 inch increases speed to just over 20,000 rpm. In neither case is this bearing practical.

Pressurized Journal Bearing. This bearing will not be practical because the flow requirement will be too large.

Conclusions. One or another bearing type does not clearly come out superior in this discussion. The three-lobe or either of the two ball bearings each have certain advantages. All are, of course, proven designs.

Three-lobe	Very low power dissipation No separate lube source Infinite storage life
Ball bearing	No volume penalty due to lube storage High reliability
Angular contact	Less radial play Greater stiffness
Deep groove	Operates at higher speed Greater selection of cages Less power loss

TABLE 2. Power Dissipation and Flow, Three-Lobe Bearing, L/D = 1.

Clearance, in.	0.001	0.0006	0.000394
Sommerfeld number	0.0085	0.024	0.055
(R/C)(F _f /W)	0.8	1.4	2.4
F _f , lb	12.8×10^{-4}	13.44×10^{-4}	15.13×10^{-4}
Q/NDLC	1.80	1.47	1.13
Q, in ³ /sec	0.094	0.046	0.023
Volume of helium gas at 400 psi, in ³	112.3	55.0	27.8
Volume of helium gas at 25,000 psi, in ³	1.80	0.88	0.44
Available volume (2 bearings), %	3.6	1.75	0.89

It would appear from this simple analysis that a ball bearing with the availability of a low viscosity lubricant may be the most desirable. How this lubricant would be stored and fed to the bearing requires a design tradeoff of the complete system.

Turbine Performance

The turbine performance potential is evaluated on the basis of the similarity parameters specific speed (N_s), Reynolds number (R_e^*), and Mach number (M_2). The specific speed is defined as

$$N_s = \frac{N\sqrt{V_3}}{H_{ad}^{3/4}} \quad (4)$$

when N denotes the rotative speed (rpm), V_3 the volumetric flow rate at rotor exit (ft^3/sec) and H_{ad} the isentropic expansion head (ft). This parameter, together with either the specific diameter

$$D_s = \frac{DH_{ad}^{1/4}}{\sqrt{V_3}} \quad (5)$$

or the turbine velocity ratio u/c_o , defines the dynamic similarity when D denotes the rotor diameter (ft), u the rotor tip speed (ft/sec) and

$$c_o = \sqrt{2gH_{ad}} \quad (6)$$

the *spouting velocity* (ft/sec). Turbine designs having the same numerical values of N_s and D_s or N_s and u/c_o have similar velocity vectors and thus the same efficiency, providing that geometric similarity is maintained and that the flow-path Reynolds numbers and Mach numbers are equal. Geometric similarity exists when certain geometric ratios, such as rotor width to rotor diameter, clearance to diameter, chord length to diameter, blade trailing edge thickness to diameter, etc. are constant. Usually certain *optimum* values for geometric ratios (e.g., chord length to diameter) exist for obtaining highest efficiencies. The flow path Reynolds number and Mach numbers are significant values for the losses and thus determine the level of efficiency. The flow-path Reynolds numbers are represented by the machine Reynolds number

$$R_e^* = \frac{uD}{\nu} \quad (7)$$

The most significant Mach number in the flow path is the Mach number, M_2 , at the nozzle exit since it governs, together with the turbine velocity ratio, the relative Mach number in the rotor channels.

Considering now that certain values of the specific diameter or turbine velocity ratios become *optimum* for given values of N_s , it is sufficient to plot the turbine efficiency against N_s for fixed values of R_e^* and M_∞ to represent the efficiency potential. Typical data are shown in Figure 10 for single stage axial partial admission turbines and single stage partial admission Terry turbines.

The diagram of Figure 10 shows that the axial turbine has the highest efficiency potential, namely 29% at a specific speed of 1, and about 50% at the specific speed of 4, whereas, the Terry turbine efficiency potential is 18 and 39%, respectively. These data assume that the Machine Reynolds number is 10^6 or higher and that the relative Mach number at rotor inlet, M_{w-2} is subsonic. The reason for the lower efficiency potential of the Terry turbine is the comparatively crude rotor bucket shape and the limited number of rotor buckets which can be placed on a rotor due to geometric limitations.

No efficiency derating is required for axial turbines when the relative Mach number is supersonic, providing that a properly shaped rotor blade (usually a converging diverging rotor channel) is used and that the leading and trailing edge thicknesses of the rotor blades are thin. Another requirement is that the number of rotor blades in the low specific speed regime is comparatively high, namely 100-160.

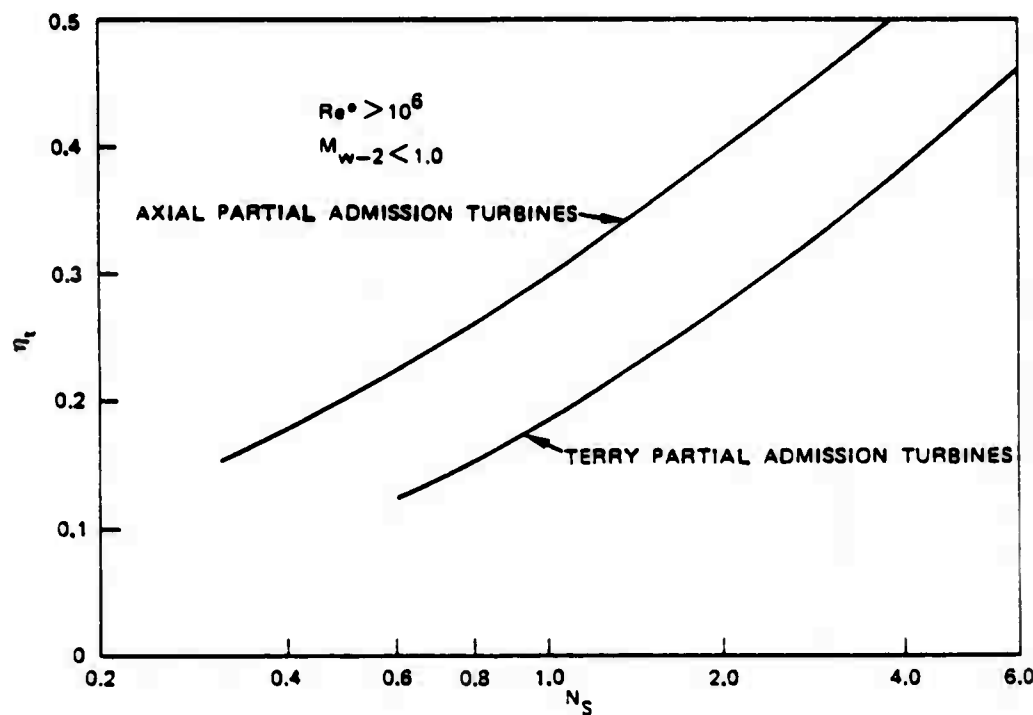


FIGURE 10. Efficiency Potential of Axial and Terry Partial Admission Turbines.

Preliminary calculations show that the machine Reynolds number for a 100-watt turbine is comparatively low, between 4×10^4 and 9×10^4 , and that the Mach number at nozzle exit is comparatively high, about 3.6, so that the relative Mach number at rotor inlet is supersonic, varying between 2 and 2.8, depending on specific speed. Thus, the data presented in Figure 10 have to be derated, particularly for the axial turbine since the likely rotor diameter is 1 inch or below, which will make it impossible to place the desired number of rotor blades or to fabricate the desired supersonic rotor channel geometry. A smaller amount of derating is required for the Terry turbine, since the rotor blade bucket of Terry turbines seems to be less sensitive to high relative Mach numbers. Figure 11 shows the derated efficiency potential for Terry turbines which is in fair agreement with test data on a small (0.5 inch) high speed Terry turbine reported in footnote 1. It has to be observed that the turbine efficiency data quoted in footnote 1 are the hydraulic efficiency (i.e., neglecting rotor windage losses) and that a comparatively wide scatter exists due to the difficulties encountered in measuring small amounts of net power (0.5-2 watts) at high rotative speeds (30,000-80,000 rpm). Correcting these data for the windage losses, Figure 12 results where the solid line represents the Terry turbine efficiency presented in Figure 11.

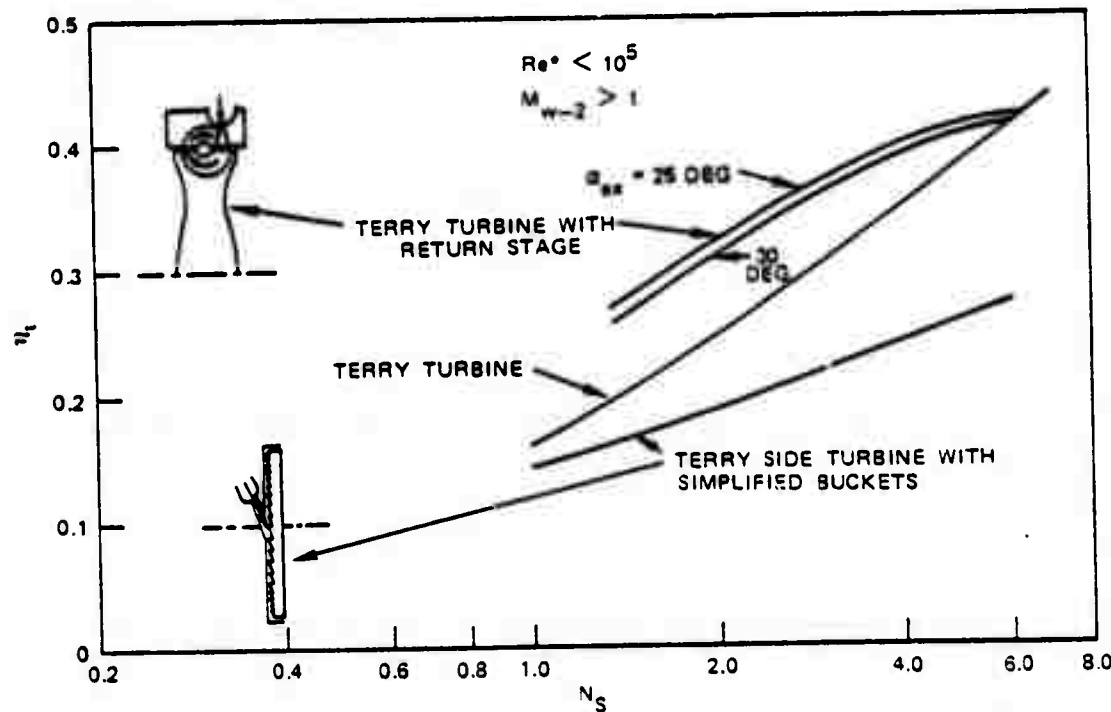


FIGURE 11. Efficiency Potential of Low Diameter, High Mach Number Turbines.

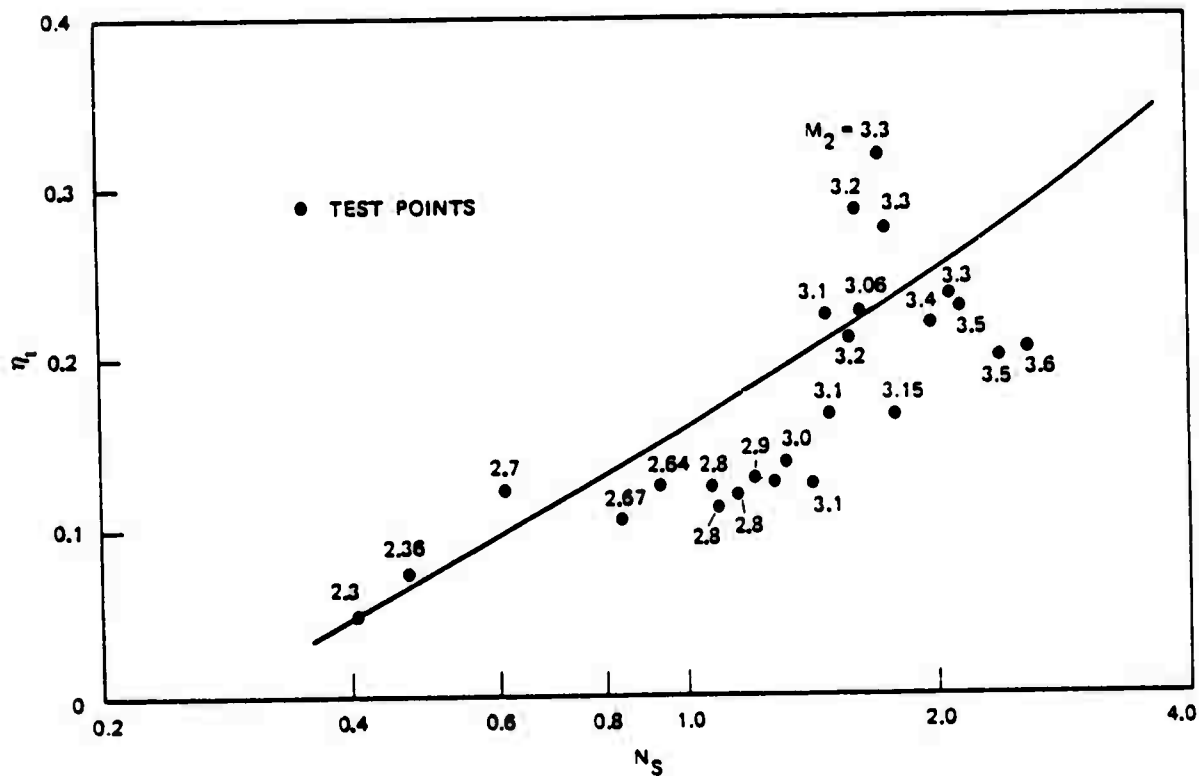


FIGURE 12. Test Data of Low Diameter, High Mach Number Terry Turbines.

Another turbine type which is frequently used for low cost, high speed power units is a modified Terry turbine with buckets at the side of the rotor disk (instead of at the rim) where the buckets are highly simplified, i.e., are merely indentations as schematically shown in the lower insert of Figure 11. This means that the reaction moment of the rotor is extremely small since the nozzle jet tends to spill over the buckets instead of being turned around by 180 degrees. Thus, the efficiency potential is significantly lower. Typical data for small ($D = 1.5\text{-}2.0$ inches) Terry turbines with side pockets are represented in the lower line in Figure 11.

It should be observed at this point that, in principle, the placement of properly shaped Terry buckets at the side of the disk does not cause an efficiency penalty, as evidenced by experimental data, provided that the rotor rim thickness is comparatively small to avoid excessive windage losses.

Examining the velocity vectors of low specific speed turbines in more detail, it is found that the leaving energy is comparatively high and can be utilized by providing a return stage which redirects the rotor exit vector toward the rotor inlet at the downstream side as schematically sketched on the upper insert of Figure 11, thus generating additional torque. Calculations show that the torque amplification, and thus efficiency increase, is primarily a function of the turbine velocity ratio, i.e., specific

speed and, to a lesser degree, a function of the return stage exit angle. These data are shown in Figure 13 by plotting the efficiency amplification factor for two different return stage exit angles, 25 and 30 degrees. Converting these data to the efficiency potential, the upper lines in Figure 11 result, which show a significant efficiency improvement at the specific speed between 1 and 4.

Unit Performance

Assuming that an electrical efficiency of 85% can be obtained and the alternator windage losses follow the trend described in Figure 1, the product of electrical efficiency, *windage efficiency*, and bearing efficiency is calculated and shown in Figure 14 as a function of rotative speed, when deep groove ball bearings are used and an oil viscosity of 10 centistokes can be realized. With these data, the overall unit efficiency is calculated using the data of Figure 11 for the turbine efficiency. These data are presented in Figures 15 through 17 and Tables 3 through 5; they show that the specific speed varies between 2 and 4 and that the overall efficiency increases with increasing rotative speeds. The turbine rotor diameters decrease with increasing rotative speeds and have values from about 1.4-0.67 inch and the nozzle exit diameter varies from 0.024-0.019 inch. Comparatively small nozzle throat diameters result (for single nozzles) varying from 0.00878-0.0116 inch. The nozzle exit Mach number, assuming impulse action, is $M_2 = 3.637$. At a rotative speed of 200,000 rpm a unit with a single stage Terry turbine, presented in Figure 15, has an overall efficiency of about 22%. Adding a reentry stage, the overall efficiency increases to 25.8% at 200,000 rpm and can reach values of 27.7% at 300,000 rpm, as shown in Figure 16. Significantly lower values are obtained with a Terry side turbine having simplified buckets, Figure 17, namely 16.9% overall efficiency at 200,000 rpm.

Somewhat lower overall efficiency values will result when an oil viscosity of 20 centistokes has to be assumed. All data assume a turbine exit pressure of 14.7 psia.

Figures 15 through 17 show that the goal of an overall efficiency of 30% cannot be obtained. A Terry turbine with one return stage shows the highest efficiency potential. Limiting its speed to 200,000 rpm to favor ample bearing life, a rotor diameter of 0.846 inch and a nozzle exit diameter of 0.0193 inch results, yielding, however, a gas consumption which is 16% higher than desired. By increasing the rotative speed to 250,000 rpm, where the bearing life may still be adequate, a rotor diameter of 0.742 inch with a nozzle exit diameter of 0.019 inch results. The gas consumption is still 11% higher than desired. For all cases, fine rotor balancing (5-10 microinch-ounces) will be required to avoid excessive bearing loads. A certain amount of development time will be required to optimize the return stage, since experimental data for the optimum return stage configuration for small units are not available. One potential problem in such development efforts will be to obtain consistent data for the turbine net output without undue data scatter.

NWC TP 6029

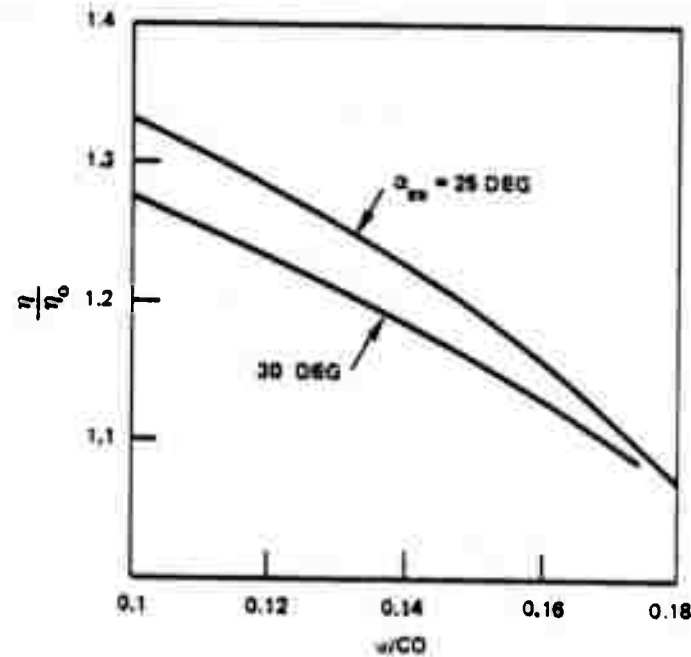


FIGURE 13. Amplification Effect of Return Stage for Terry Turbines.

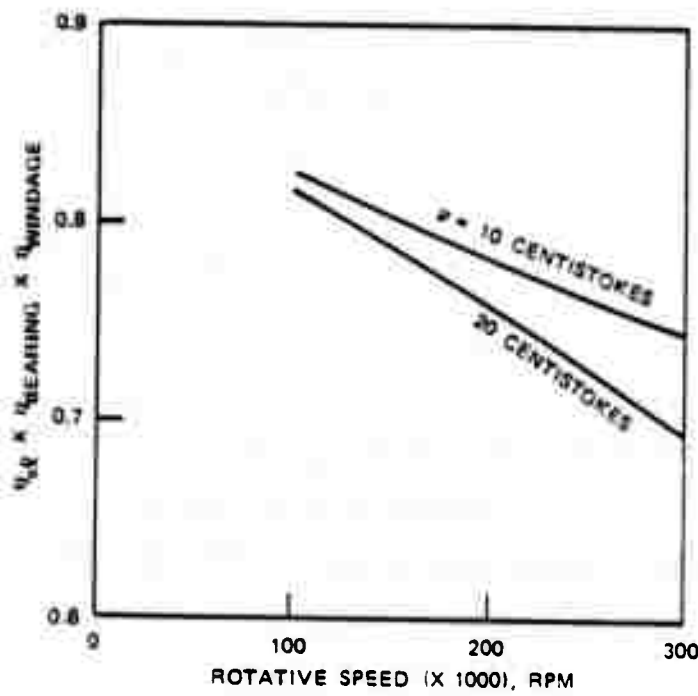


FIGURE 14. Product of Electrical and Mechanical Efficiency.

NWC TP 6029

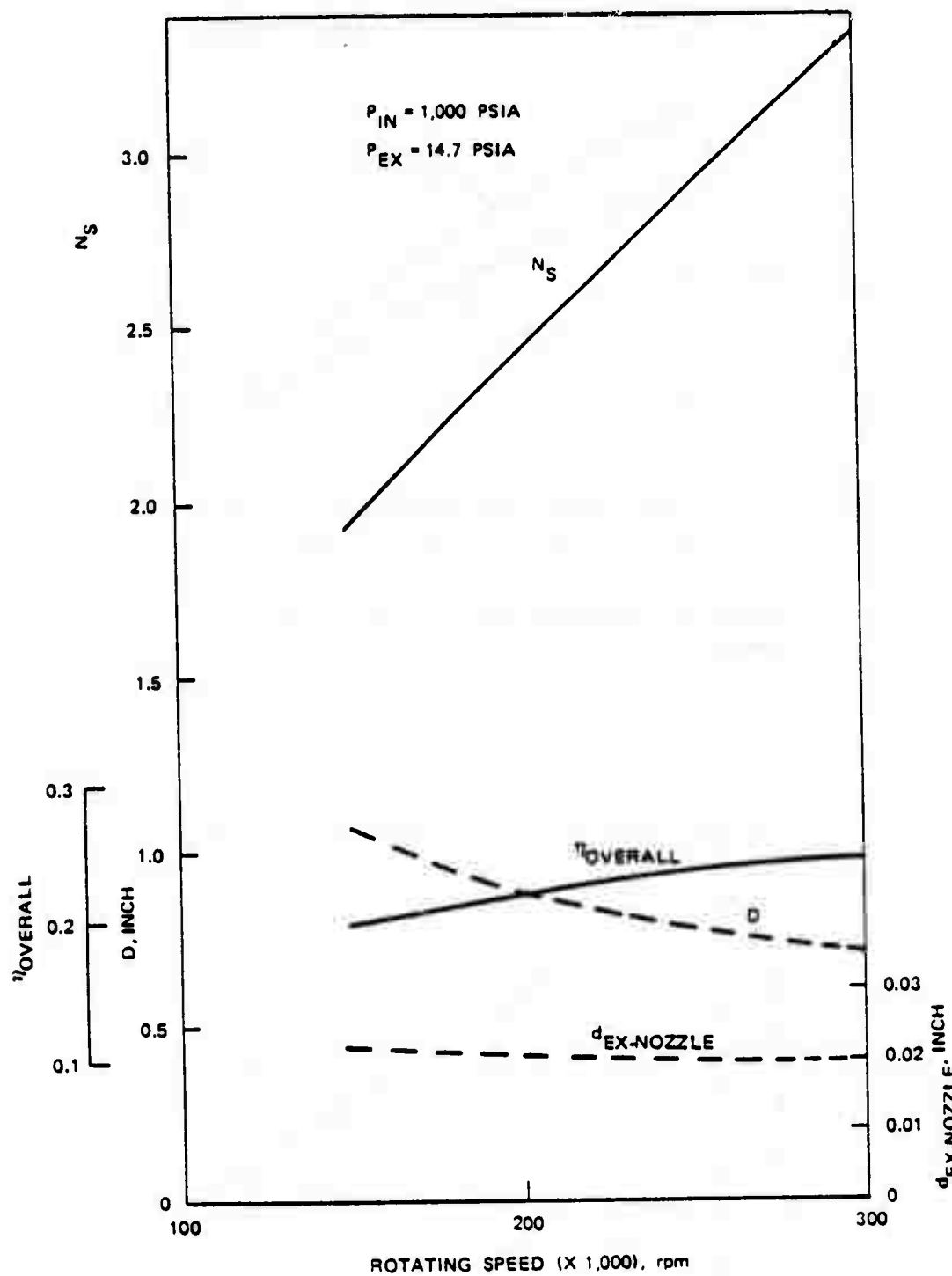


FIGURE 15. Helium Unit Performance Data When Using Terry Turbines.

NWC TP 6029

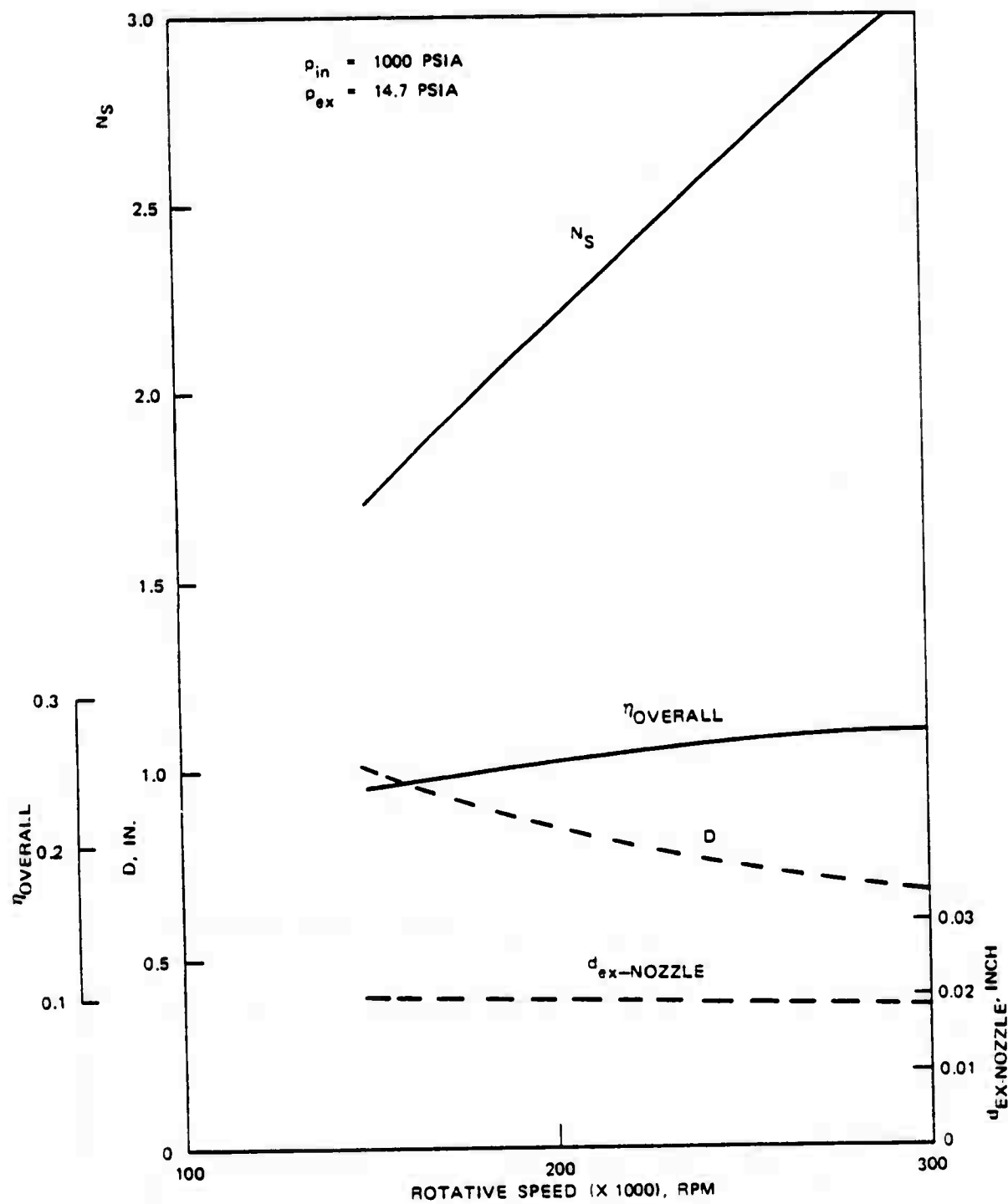


FIGURE 16. Helium Unit Performance Data When Using Terry Turbine With Return Duct.

NWC TP 6029

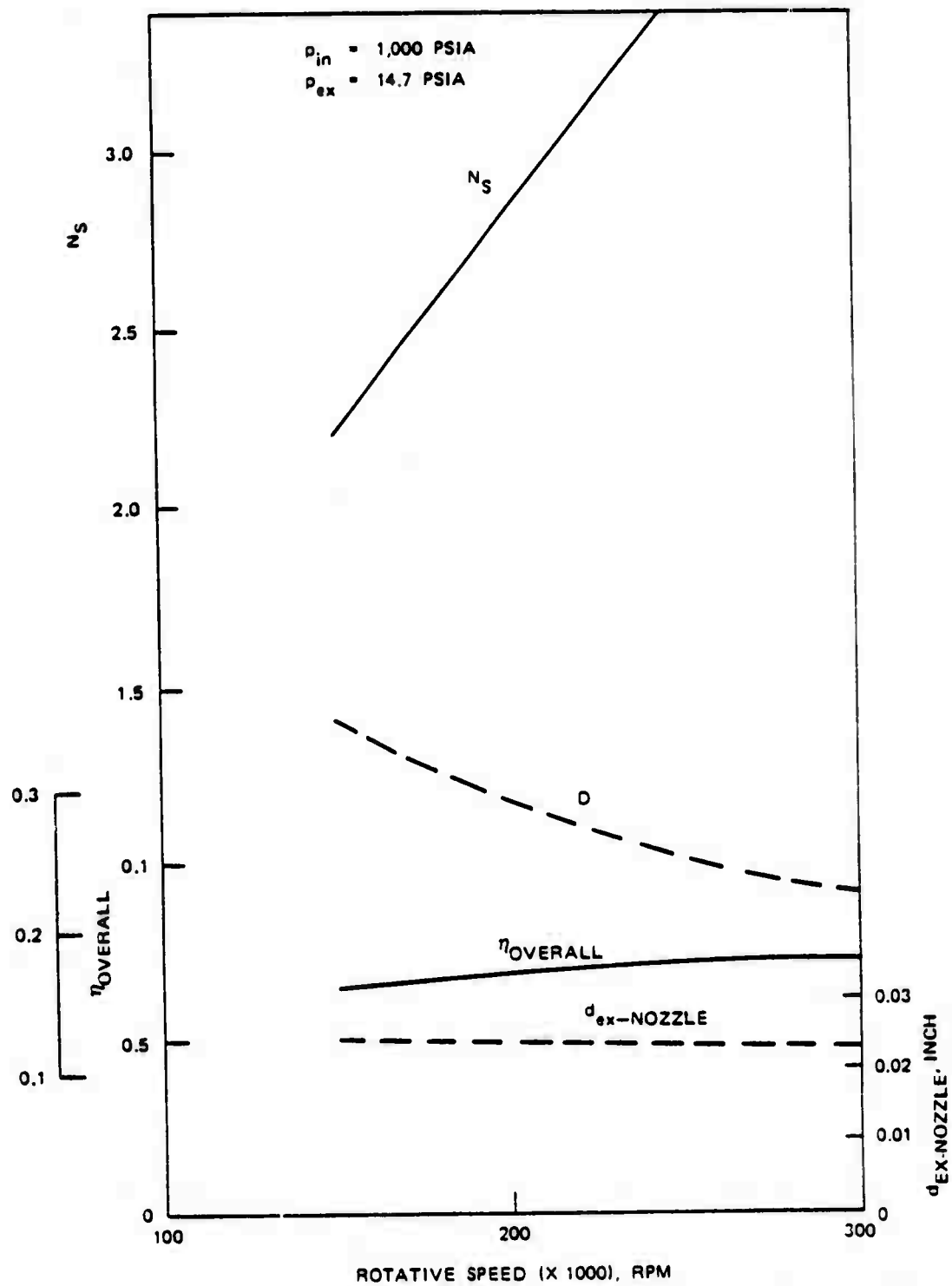


FIGURE 17. Helium Unit Performance Data When Using Terry Side Turbine With Simplified Rotor Buckets.

NWC TP 6029

TABLE 3. Unit Performance Data, Terry Turbine, Helium.

	Rotative speed (N), rpm			
	150,000	200,000	250,000	300,000
η_t	0.2446	0.2777	0.3045	0.3257
$\eta_{overall}$	0.197	0.218	0.233	0.2426
N_s	1.93	2.407	2.877	3.335
u/c_0	0.117	0.1302	0.1419	0.1524
D, inch	1.071	0.8942	0.7798	0.6982
R _e [*]	44947	43210	42227	41626
W, lb/sec	0.000668	0.000604	0.000566	0.000543
d _{throat} , inch	0.010393	0.00989	0.009584	0.009374
M ₂	3.637	3.637	3.637	3.637
d _{ex-nozzle} , inch	0.0221	0.02104	0.02039	0.01994

TABLE 4. Unit Performance Data, Terry Turbine with Re-entry, Helium.

	Rotative speed (N), rpm			
	150,000	200,000	250,000	300,000
η_t	0.296	0.3296	0.3533	0.3722
$\eta_{overall}$	0.238	0.2587	0.27	0.277
N_s	1.708	2.149	2.598	3.044
u/c_0	0.11	0.123	0.135	0.1458
D, inch	1.009	0.846	0.742	0.668
R _e [*]	42137	40938	40399	40124
W, lb/sec	0.000552	0.000509	0.000489	0.000476
d _{throat} , inch	0.00945	0.00908	0.008896	0.00878
M ₂	3.637	3.637	3.637	3.637
d _{ex-nozzle} , inch	0.0201	0.0193	0.01892	0.01868

TABLE 5. Unit Performance Data, Terry Side Turbine with Simplified Buckets, Helium.

	Rotative speed (N), rpm			
	150,000	200,000	250,000	300,000
η_t	0.198	0.2156	0.2295	0.2406
$\eta_{overall}$	0.159	0.169	0.1755	0.1793
N_s	2.204	2.818	3.436	4.06
u/c_0	0.1525	0.1688	0.1832	0.1964
D, inch	1.397	1.16	1.007	0.8993
R, °	42904	68238	65214	63078
W, lb/sec	0.00083	0.000777	0.00075	0.000735
d _{throat} , inch	0.01159	0.01121	0.01102	0.010908
M ₂	3.637	3.637	3.637	3.637
d _{ex-nozzle} , inch	0.0247	0.02386	0.02343	0.0232

Sketches for the detailed geometry of a turbine design operating at 200,000 rpm are provided in Figures 18 and 19.

A Terry turbine without return stage will need a gas supply which is 38% higher than the design goal when operating at 200,000 rpm or a gas supply which is 29% higher than design goal when operating at 250,000 rpm. The advantage of this design version is the elimination of the return stage, i.e., a lower cost turbine design.

A Terry turbine with simplified side buckets will reduce the turbine cost even further but needs a gas supply which is 78% higher than design goal when operating at 200,000 rpm or 71% higher than design goal when operating at 250,000 rpm.

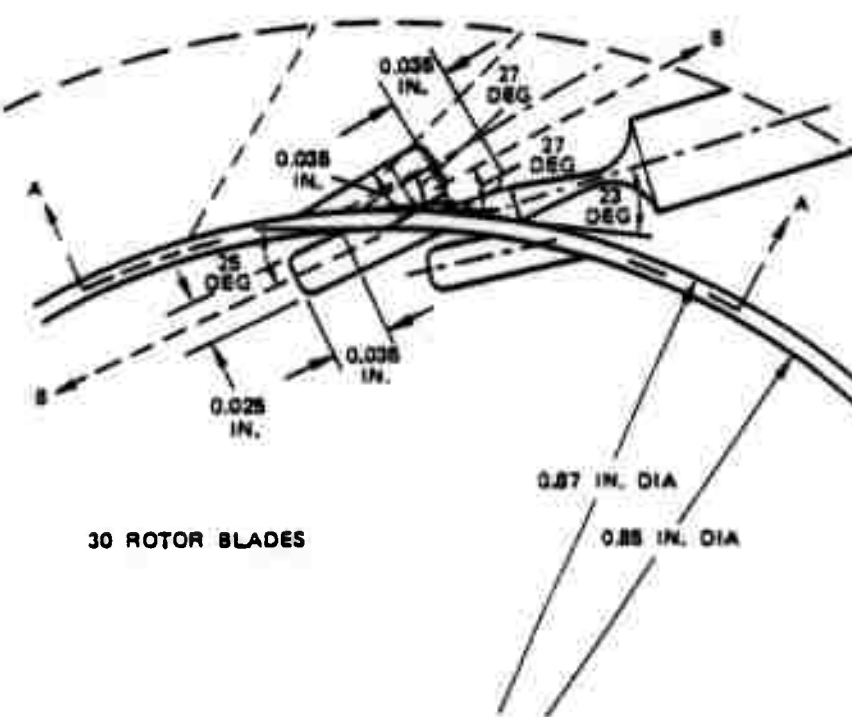
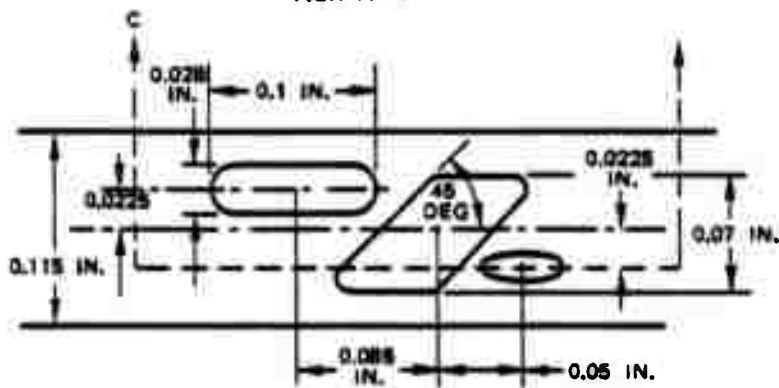
NITROGEN SYSTEM

Scope of Investigations

A nitrogen system will have many similarities with the previously discussed helium system, the main differences being the alternator type, the operating speed, and the working fluid. It appears from the available information that typical flux switch alternators have an efficiency of about 80% at 50,000 rpm and that the efficiency decreases with increasing speed as indicated in Figure 20. It is assumed that ball bearings are used and that the power absorption data of deep groove ball bearings presented in Figure 2 are applicable. A viscosity of 20 centistokes is used for the study. The turbine performance data shown in Figure 11 are also applicable.

NWC TP 6029

VIEW A-A



30 ROTOR BLADES

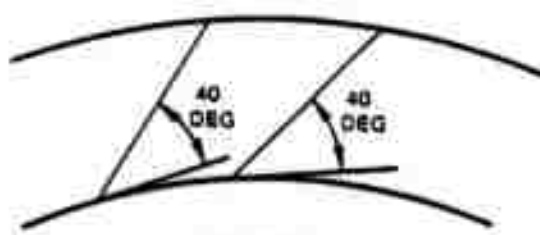
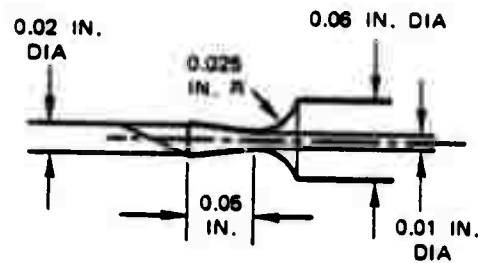
SECTION C-C

SECTION B-B

FIGURE 18. Turbine Design Data (Helium System).

NWC TP 6029

NOZZLE DETAILS



EXIT PORT

FIGURE 19. Turbine Design Details (Helium System).

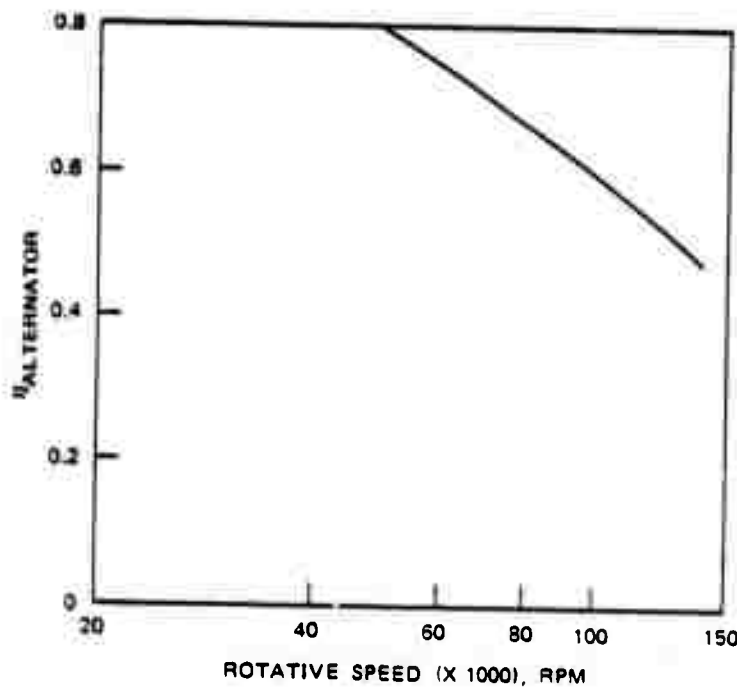


FIGURE 20. Flux Switch Alternator Performance Data (Nitrogen System).

Unit Performance

Overall performance data have been calculated for three different turbine types: the Terry side turbine with simplified buckets, the Terry turbine, and the Terry turbine with return stage. The calculated data are presented in Tables 6 through 9 for rotative speeds of 50,000 and 60,000 rpm, using the alternator performance data presented in Figure 20, and for the assumption that an alternator efficiency of 80% can be obtained at 60,000 rpm. The salient performance data are shown in Figure 21 by plotting the flow rates and overall efficiency as functions of speed for the different turbine types. The solid lines in this diagram represent the data resulting when the alternator efficiency curve follows the trend data presented in Figure 20, whereas the dashed lines assume that the alternator efficiency at 60,000 rpm is 80%. As it was to be expected, the Terry side turbine with simplified buckets will require the highest flow rates and will obtain the lowest overall efficiency, whereas the Terry turbine with return stage having a value of $\alpha_{ex} = 25$ degrees requires the lowest flow rates and obtains the highest overall efficiency. These data also show that in cases where an alternator efficiency of 80% can be retained for all speeds, a slight performance gain results for the higher rotative speed, whereas for the assumed alternator efficiency trend data, about the same overall efficiency results for either speed.

A rotative speed of 60,000 rpm and a Terry turbine with return stage and $\alpha_{ex} = 27$ degrees has been selected for the assumption that the alternator trend data follow the information presented in Figure 20. Sketches for the detailed geometry of this design are presented in Figure 22. The calculated flow rate is 0.00353 lb/sec and the overall efficiency is $\eta_{overall} = 0.2576$.

**TABLE 6. Unit Performance Data, Terry Turbine,
Nitrogen.**

	Rotative speed (N), rpm		
	50,000	60,000	60,000
	$\eta_{alternator}$	0.8	0.75
η_t	0.276	0.299	0.297
$\eta_{overall}$	0.218	0.226	0.234
N_s	2.383	2.78	2.737
u/c_o	0.129	0.1395	0.1385
D, inch	1.355	1.217	1.2
$R_e^* (X 10^5)$	1.97	1.95	1.91
W, lb/sec	0.00416	0.004013	0.00389
d_{throat} , inch	0.01575	0.0154	0.0152
M_2	3.42	3.42	3.42
$d_{ex-nozzle}$, inch	0.0395	0.039	0.0381

TABLE 7. Unit Performance Data, Terry Turbine
with Re-entry, $\alpha_{ex} = 25$ deg, Nitrogen.

	Rotative speed (N), rpm		
	50,000	60,000	60,000
	$\eta_{alternator}$		
	0.8	0.75	0.8
η_t	0.329	0.3538	0.3498
$\eta_{overall}$	0.26	0.263	0.2753
N_s	2.13	2.52	2.468
u/c_0	0.1226	0.133	0.132
D, inch	1.28	1.16	1.1486
$R_e^* (X 10^5)$	1.85	1.86	1.81
W, lb/sec	0.00349	0.003466	0.0033
d_{throat} , inch	0.0144	0.0144	0.014
M_2	3.42	3.42	3.42
d_{exit} , inch	0.0362	0.036	0.0352

TABLE 8. Unit Performance Data, Terry Turbine
with Re-entry, $\alpha_{ex} = 30$ deg, Nitrogen.

	Rotative speed (N), rpm		
	50,000	60,000	60,000
	$\eta_{alternator}$		
	0.8	0.75	0.8
η_t	0.317	0.34	0.336
$\eta_{overall}$	0.25	0.252	0.2645
N_s	2.184	2.585	2.535
u/c_0	0.124	0.1347	0.133
D, inch	1.3	1.175	1.164
$R_e^* (X 10^5)$	1.88	1.88	1.84
W, lb/sec	0.00363	0.0036	0.003447
d_{throat} , inch	0.0147	0.0146	0.0143
M_2	3.42	3.42	3.42
d_{exit} , inch	0.0369	0.0368	0.036

TABLE 9. Unit Performance Data, Terry Side
Turbine with Simplified Buckets, Nitrogen.

	Rotative speed (N), rpm		
	50,000	60,000	60,000
	$\eta_{\text{alternator}}$		
	0.8	0.75	0.8
η_t	0.215	0.227	0.2255
η_{overall}	0.1678	0.169	0.1775
N_s	2.797	3.32	3.244
u/c_o	0.168	0.18	0.179
D, inch	1.76	1.575	1.56
$R_e^* (X 10^5)$	3.16	3.07	3.0
W, lb/sec	0.00544	0.00538	0.00513
d_{throat} , inch	0.018	0.0179	0.0175
M_2	3.42	3.42	3.42
d_{exit} , inch	0.0451	0.0449	0.0439

NWC TP 6029

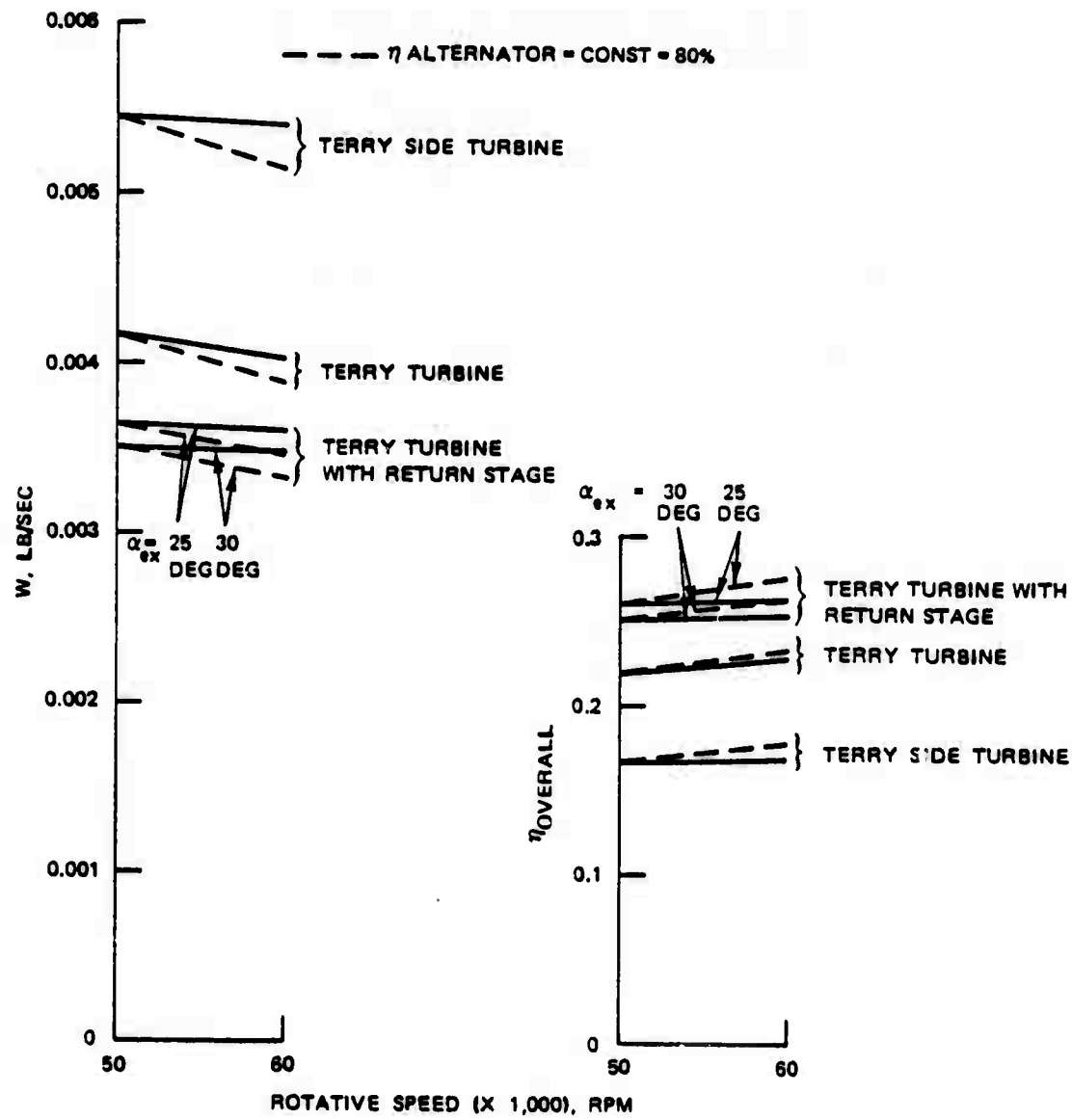


FIGURE 21. Nitrogen System Performance Data.

NWC TP 6029

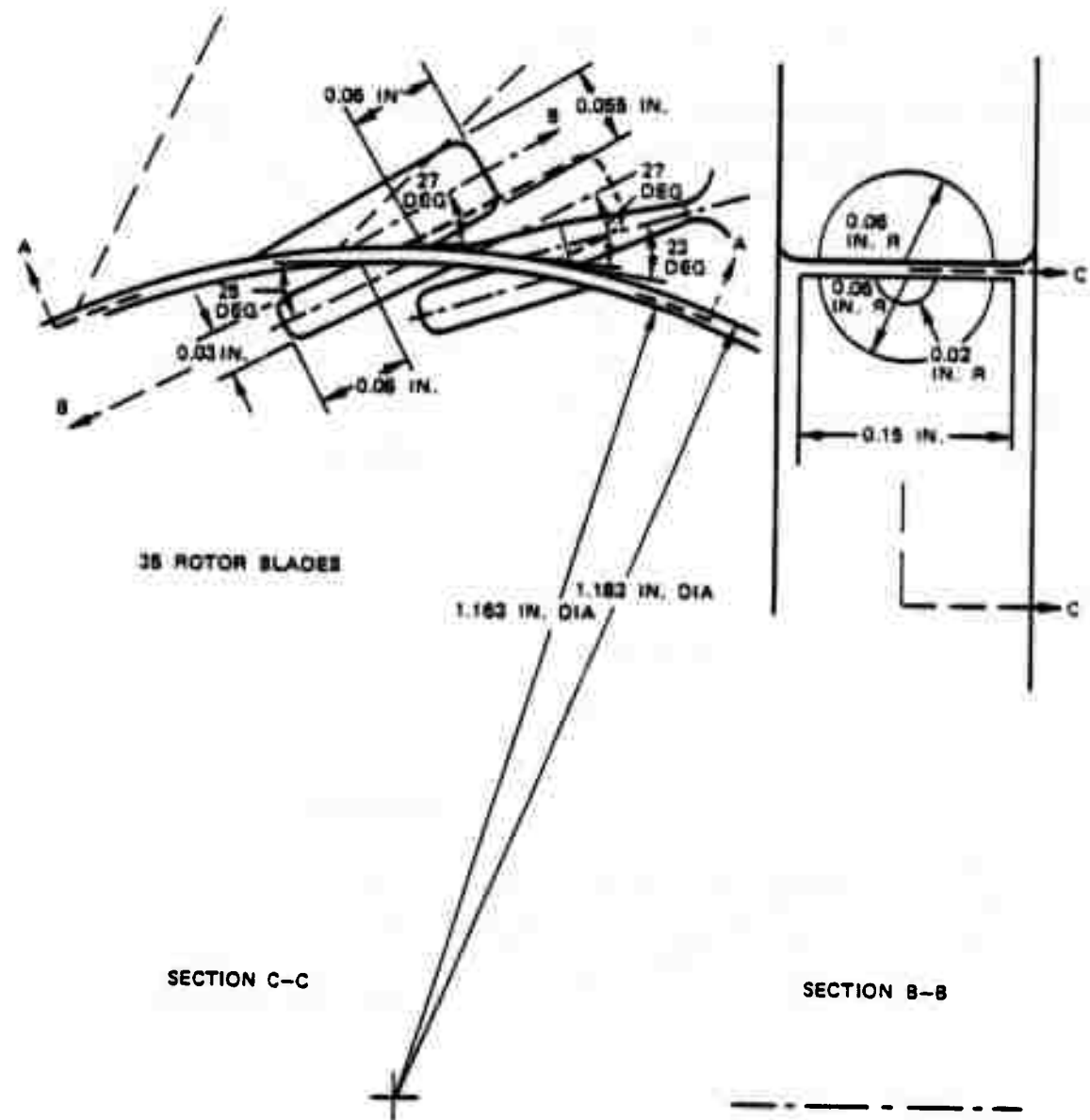
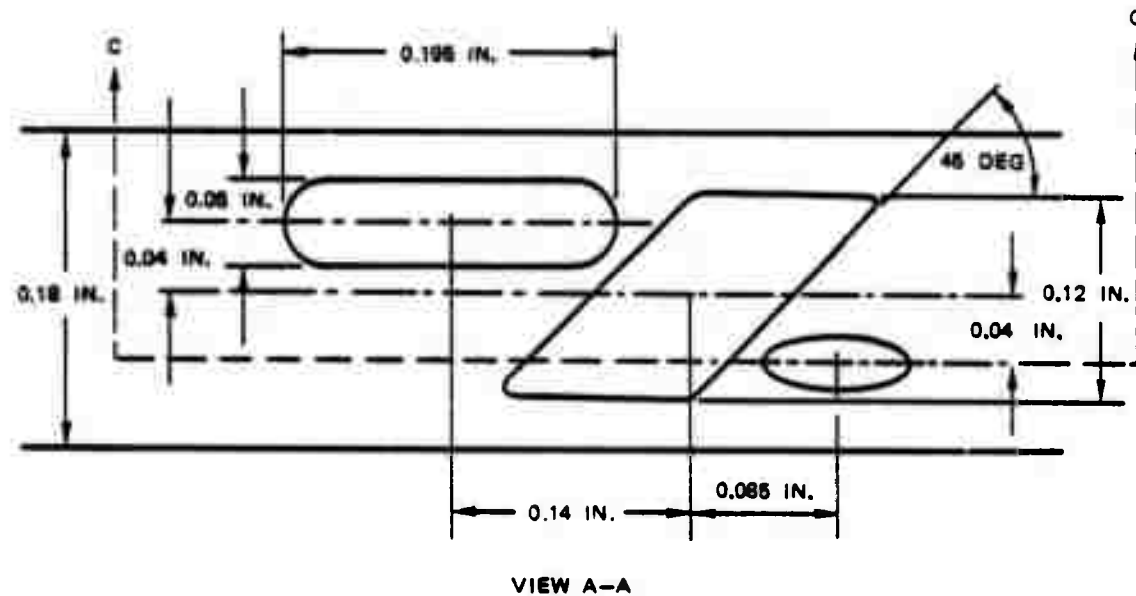


FIGURE 22. Turbine Design Data (Nitrogen System).

NWC TP 6029



VIEW A-A

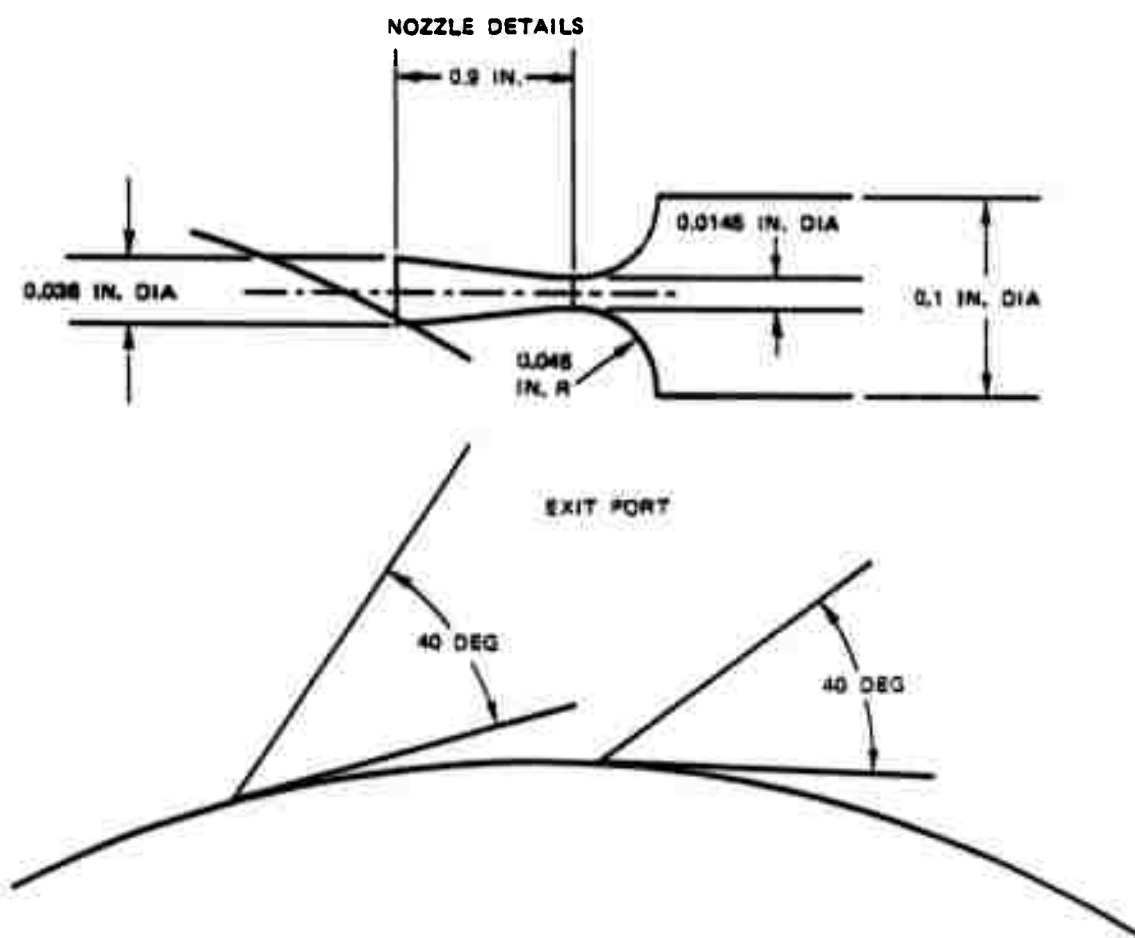


FIGURE 22. (Contd.)

SUMMARY**HELIUM SYSTEM**

Examination of the few available data on the electrical efficiency of high speed, low power alternators shows that test data are not well documented, but that an electrical efficiency of 85% does not seem to be unreasonable. By keeping the alternator rotor diameter small, speeds up to 275,000 rpm appear to be possible.

Investigations on bearings lead to the conclusion that three-lobe gas fed journal bearings have a comparatively low gas consumption and power absorption, but that extremely small tolerances have to be maintained, thus indicating comparatively high cost. Miniature precision ball bearings are feasible to rotative speeds of about 250,000 rpm but need an oil supply either by packing the bearing with grease or by providing an oil supply and feeding the bearing with a wick. A low viscosity oil is desired to favor low power absorption.

A Terry turbine with a return stage should be applied to obtain high turbine efficiencies. Even then the desired overall efficiency goal is not obtained. The gas supply has to be increased by 11% for a 250,000 rpm unit and by 16% for a 200,000 rpm unit. A Terry turbine without return stage will need a gas supply which is 38% higher than design goal when operating at 250,000 rpm. A low cost Terry turbine with simplified side buckets will need a gas supply which is 78-71% in excess of the goal.

An experimental development program will be required for the Terry turbine reentry stage, where measuring the comparatively small net output at the high rotative speed will require special test fixtures.

The deep groove ball bearing would appear to be adequate but will need a grease or oil supply which may cause shelf life problems. To avoid excessive bearing loads, i.e., to obtain adequate bearing life, fine rotor balancing will be required.

NITROGEN SYSTEM

The helium unit selected has a rotative speed of 200,000 rpm, a turbine rotor diameter of 0.85 inch, a flow rate of 0.000509 lb/sec, and a projected overall efficiency of 0.2587. The recommended nitrogen unit has a speed of 60,000 rpm, a flow rate of 0.00353 lb/sec, and about the same overall efficiency with a rotor diameter of 1.163 inches, i.e., has a weight flow rate which is about seven times higher. For both cases a Terry turbine with return stage was found to be the most efficient design configuration.

INITIAL DISTRIBUTION

18 Naval Air Systems Command

AIR-03B (1)
AIR-03P2 (1)
AIR-320 (1)
AIR-340B (1)
AIR-350F (1)
AIR-503 (1)
AIR-510B (1)
AIR-5108 (1)
AIR-5109 (1)
AIR-5203 (1)
AIR-52032C (1)
AIR-5312 (1)
AIR-53232 (1)
AIR-5332 (1)
AIR-5351 (1)
AIR-5366 (1)
AIR-954 (2)

4 Chief of Naval Material

MAT-030 (1)
MAT-032 (1)
NSP-27 (1)
NSP-2731 (1)

10 Naval Sea Systems Command

SEA-03 (1)
SEA-031 (1)
SEA-033 (1)
SEA-09B4 (4)
SEA-09G32 (2)
SEA-6531 (1)

1 Air Test and Evaluation Squadron 5

1 Naval Air Development Center, Warminster (SEVN)
1 Naval Intelligence Support Center (OOXA, Jack Darnell)
1 Naval Ocean Systems Center, San Diego (Code 133)
1 Naval Ordnance Station, Indian Head (Code FS, A. T. Camp)
1 Naval Surface Weapons Center, Dahlgren Laboratory, Dahlgren (Code DF12, Ken Baile)
3 Naval Surface Weapons Center, White Oak
 Code 33, H. Heller (1)
 Code G. C. W. Bernard (1)
 Code GW (1)
1 Naval Intelligence Support Center Liaison Officer (LNN)
4 Army Armament Materiel Readiness Command (AMSAR-SF)
4 Army Armament Research and Development Center (SMD, Concepts Branch)

4 Air Force Systems Command, Andrews Air Force Base

DL (1)

DLPI (1)

DLW (1)

SDW (1)

2 Air Force Aero-Propulsion Laboratory, Wright-Patterson Air Force Base

RJA (1)

STIMSO (1)

5 Air Force Armament Laboratory, Eglin Air Force Base

DLD (1)

DLI (1)

DLM, Capt. Aden (1)

DLO (1)

DLQ (1)

1 Foreign Technology Division, Wright-Patterson Air Force Base (Code PDMA, James Woodard)

1 Wright-Patterson Air Force Base (Code XRHP)

1 Defense Advanced Research Projects Agency, Arlington

2 Defense Documentation Center